Performance Analysis of the Phonocardiography and Seismocardiography Systems in Various Real-life Scenarios

As discussed in Chapter 2, analysis of the heart sound signal provides crucial diagnostic information about various cardiovascular pathologies [Kwak and Kwon, 2012; Choi and Jiang, 2008; Elgendi et al., 2014]. Therefore, analysis of such signal is of paramount importance, and PCG and SCG are the two existing systems are used for this purpose. PCG uses a sensor called stethoscope to acquire the acoustic sounds produced by the movement of the heart valves. On the other hand, SCG uses a sensor called accelerometer to acquire precordium vibrations. However, both the signals are vulnerable to environmental noises as well as noises generated due to the motion of the subject and noise generated due to the movement of other organs such as lungs. In literature, various methods have been proposed to address the issues related to denoising of the PCG and SCG signal, but separately. The performance of both the systems in the presence of noise is crucial to show their applicability in real-life scenarios. Therefore, the performance of both the PCG and SCG systems are analysed simultaneously in various real-life scenarios.

3.1 INTRODUCTION

PCG is the most widely used cardiography technique for heart sound signal analysis [Jain and Tiwari, 2014]. It uses a transducer called stethoscope, which amplifies the sound. Working principle of the stethoscope is briefly described in Section 3.2. It has adequate sensitivity to acquire heart sound signal [Shen et al., 2013]. Despite of its diagnostic capabilities, PCG has been long overlooked by medical fraternities because its signal is highly susceptible to various types of noises [Gradolewski and Redlarski, 2014; Naseri et al., 2013]. This deficiency of PCG limits its use for heart monitoring at home and in many real-life scenarios. Another deficiency of PCG for long-term monitoring is the large size and heavy weight (typically 40 mm diameter and 90 gm weight) of its sensor i.e. stethoscope. Although PCG system can be a natural choice due to ease of operation, it still needs to be improved in term of its size and weight. As a result of the above-mentioned deficiencies of the PCG, a cardiography system is required which is robust to noise and convenient for patients to wear while long-term monitoring.

Another method to analyse the heart sound signal is based on SCG. It uses a sensor called accelerometer to measure the precordial vibration signals, from which the heart sound signal can be extracted [Hu et al., 2014; Tavakolian et al., 2013]. Recently emerged MEMS technology based accelerometers are small in size and low in weight (typically 3(L) x 5(W) x 1(H) mm size and <3gm in weight) [Metropolia, 2014]. Section 3.2 provides brief description of working principle of a MEMS accelerometer. These accelerometers have high sensitivity and accuracy. Furthermore, MEMS accelerometers have a linear frequency response [Albarbar et al., 2009; Acar and Shkel, 2003]. The SCG signal is composed of high-frequency components and low-frequency components [Castiglioni et al., 2007]. The high and the low frequency components are generated due to closure of the heart valves and due to recoil forces,

respectively. The heart sound signal has been extracted from the high-frequency components [Tavakolian et al., 2013].

Thus, due to small size and low weight of the accelerometer, SCG is a convenient system to wear. Rienzo et al. [Rienzo et al., 2013a] developed a wearable system to record SCG signal for long-term monitoring in out-of-clinic environment. The signal was recorded while the subject was travelling on a train. However, for analysis, only those portions of the signal were considered when the subject was not in motion i.e. motionless segment. This separation requires manual intervention. Furthermore, the impact of various noises, which occur in real-life scenarios (including motion of the subject), on the recorded signal was not analysed.

Henceforth, in this chapter, a performance analysis of both the PCG and SCG systems in real-life scenarios is provided. For this purpose, both PCG and SCG signals were simultaneously acquired in real-life scenarios, i.e. subject is 'in meeting', 'walking', 'travelling', 'in motion' and 'in market'. These scenarios are likely to happen in daily-life and prone to have noise sources. ECG signal is also acquired to use as a reference signal, simultaneously to the PCG and SCG signal. To compare the performance of both the systems quantitatively, the detection rate of S1 and S2, and number of false points are obtained for each scenario. Furthermore, a quality index based on the energy of the FHS and the rest of the cycle is proposed and obtained. The quality index analyses the robustness of the PCG and the SCG systems against various noises.

The chapter is organised as follows. The working principles of stethoscope and accelerometer are provided in Section 3.2. Section 3.3 illustrates the developed system setup for signal acquisition. The acquired PCG and SCG signals are analysed in the time, frequency, and time-frequency domain, described in the Section 3.4. Results and discussion of the comparative performance analysis of both PCG and SCG systems are provided in Section 3.5.

3.2 WORKING PRINCIPLE OF STETHOSCOPE AND ACCELEROMETER

PCG and SCG are two existing methods to acquire the heart sound signal. Working principle of both the sensors stethoscope and accelerometer used in PCG and SCG respectively, are described as follows:

3.2.1 Stethoscope

PCG uses a stethoscope and a microphone, as shown in Figure 3.1, for the recording of heart sound signal. The stethoscope acquires the heart sound by placing the chest-piece on the chest wall of the subject. Movement of the heart causes vibration on the chest wall, and consequentially the air in the chest-piece vibrates. Vibration of the air generates variable acoustic pressure, which travels via the rubber tube filled with air, to the medical person's ear and perceived as sound [blurtit]. Thus, the heard sounds contain the relative information about the functionality of the heart.

As shown in Figure 3.1, the chest-piece consists of two sides that can be placed on the chest wall; one is bell and another one is a diaphragm [Callahan et al., 2007; Williams, 1874]. The bell side consists of a hollow cup, and it is useful in picking up low frequency heart sounds. When the bell side is placed on the chest wall, the acoustic pressure waves produced due to the vibrations of the air, travel up to the rubber tube. Another side of the chest-piece consists of a diaphragm, which is a flat hard disc of plastic, is meant for picking up high-frequency heart sounds. When it is placed on the chest wall, movement of the heart vibrates the diaphragm. The vibrations of diaphragm move the air in the air column up and down. Since the surface area of the diaphragm is much larger than the cross-sectional area of the air

column, the air in the tube travels a more distance than it moves in the chest-piece. It causes a magnification of the pressure waves and consequentially the sound level is magnified.

The heart sound picked from either side of the chest piece passes through the rubber tube. To convert the sound signal into an electrical signal, a microphone is placed at the end of the tube.
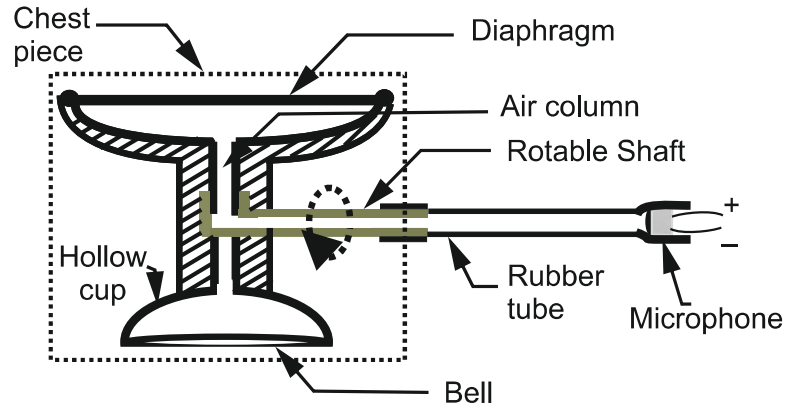

Figure 3.1 : Schematic diagram of the stethoscope

3.2.2 Accelerometer

In the SCG, an accelerometer is used to measure the acceleration caused by the motion of the heart [Jerosch-Herold et al.]. Different types of accelerometers have been developed, including piezoelectric, electromechanical servo, liquid tilt, and piezo-resistive [control learn zone, 2008]. In recent years, MEMS accelerometers have made tremendous advances in terms of its cost and level of on-chip integration [Sun et al., 2010; Metropolia, 2014]. The MEMS accelerometer is based on the principle of capacitance differentiation. These accelerometers have high sensitivity and accuracy.

A typical MEMS accelerometer is shown in the Figure 3.2. It is a typical one-axis accelerometer which can be upgraded to 2 or 3-axis by placing more sets of capacitors in 90 degrees to each other. It consists of a movable proof mass that is connected to a mechanical suspension system (spring). This setup of the mass and the spring build a mass-spring system. According to Newton's second law, if a mass, 'm_s', is undergoing with an acceleration of 'a' then there would be a force, 'F', acting on the mass with the magnitude of

$$F = m_s a \tag{3.1}$$

Another law, Hooke's law states that if a spring with spring constant δ is extended to position x from its equilibrium position, x_0, then there will be a force acting on the spring given by [Geng et al., 2013]:

$$F = \delta \Delta x \tag{3.2}$$

where $\Delta x = x - x_0$. Thus, according to Eq.(3.2), the force applied on the proof-mass displaces it proportionally. By equating equations Eq.(3.1) and Eq.(3.2); we have

$$m_s a = \delta \Delta x <=> a = (\delta \Delta x)/m_s \tag{3.3}$$

The above equation describes the relation between the acceleration of the proof-mass and the displacement in the spring.

When a mass-spring system undergoes with an acceleration, it exhibits oscillations at some characteristic natural frequency. This natural frequency is given by [Hu et al., 2014]:

$$f = \frac{1}{2\pi}\sqrt{\frac{\delta}{m_s}} \tag{3.4}$$

where f is natural frequency in Hz, δ is the spring constant in N/m, m_s is mass in Kg.

As shown in Figure 3.2, MEMS accelerometer has movable plates and the fixed outer plates and these plates are parallel to each other. Such arrangement of the plates act as the capacitor plates. In general, capacitance, 'C', between any two parallel plates governed by the following equation:

$$C = \frac{\varepsilon Ar}{d} \tag{3.5}$$

where ε is the permittivity of the plate-separating material, Ar is area of the plates, and d is the distance between the plates. A change in the values of ε, Ar or d will result in a change of the capacitance value. Using this, if the ε and Ar are known, then the d can be determined by the measured value of C.

When an acceleration is applied to the accelerometer, the proof mass moves and produces Δx displacement in the spring, according to Eq.(3.3). This displacement in spring change the distance between the plates, and this change is reflected in the change in the capacitance values such as C_A and C_B shown in Figure 3.2. If the device is at rest, and the spacing between the plates is d, then each of the capacitors exhibits a capacitance as given in Eq.(3.5). If the middle plate is moved by a distance d_0, then this results in a change of capacitance between plates as:

$$C_A = \frac{\varepsilon A}{d + d_0} \tag{3.6}$$

and

$$C_B = \frac{\varepsilon A}{d - d_0} \tag{3.7}$$

then the difference between the two capacitance is given by:

$$\Delta C = \varepsilon A \left[\frac{1}{d + d_0} - \frac{1}{d - d_0} \right] = (\varepsilon A)\frac{-2d_0}{d^2 - d_0^2} \tag{3.8}$$

For small values of displacement d, the above expression reduces to:

$$\Delta C \approx \frac{1}{d_0} \tag{3.9}$$

The change in acceleration unbalances capacitor plate distance, observed by modulation or demodulation circuits and thus, resulted in output proportional to acceleration.

3.3 SYSTEM SETUP FOR SIGNAL ACQUISITION

For experimental work, signals were acquired from five young and healthy subjects with an average weight of 80 kg, an average height of 174 cm, and an average age of 27 years. The young and healthy subjects were chosen so that the acquired signal contains FHS only and not murmur sounds. By doing this impact of noise on the signal can be analysed precisely.

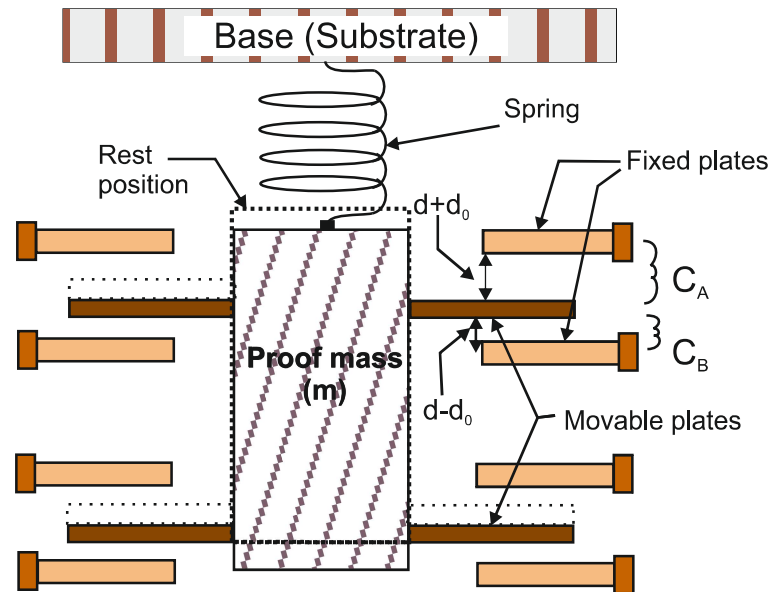A system is developed to acquire ECG, PCG and SCG signals simultaneously. The

Figure 3.2 : Schematic diagram of the MEMS accelerometer

amplitude range of the acquired signals is ± 1 Volt, same as the operating range of the sound card (3.5 mm audio input jack) on a Personal Computer (PC). The sound card significantly attenuates input signal below 10 Hz [Jason M.]. However, this feature is favourable to record the heart sound signal as, in this frequency range, it is observed that noise component has dominance over the heart sound signal. Hence, the acquired signals are stored applied to the PC through the sound card. The applied signal to the PC is converted from analog form into digital form using the inbuilt ADC of the PC and thus the system does not require external ADC. The sampling rate for the conversion was set to 1 KHz. 1 KHz sampling rate is adequate for heart sound signal because its fundamental components lie below the frequency 500 Hz [Boutana et al., 2011].

Hence the proposed system setup is simple to implement and due to use of sound card, it does not require external ADC and hence cost of ADC is eliminated. Further, such type of system can be used to acquire the heart sound signal into a smartphone (mobile phone) di-
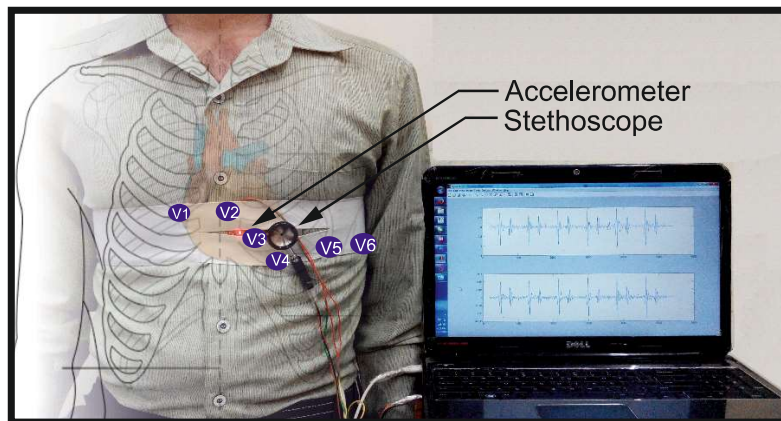

Figure 3.3 : Heart sound signal acquisition using PCG and SCG systems

rectly without need of ADC or micro-controller. The set-up for ECG, PCG, and SCG methods are described in the following subsections.

3.3.1 PCG Signal Acquisition

The stethoscope was placed at V_3 position (close to the apex of the heart), as shown in Figure 3.3. The sound signal acquired from the stethoscope has to be converted into an electric form for recording and for further processing. An electret condenser microphone is used to convert the acquired sound signal into an electrical signal. Then, the output of the microphone is connected to the PC through the sound card, as shown in Figure 3.4.

3.3.2 SCG Signal Acquisition

For the SCG, A widely used placement has been on the sternum [Inan et al., 2015]. However, Pandia, et al. [Pandia et al., 2012] found that the second heart sound was more pronounced when the SCG was measured on the left side of the chest compared to the sternum. Therefore, the accelerometer is attached to the left side of the chest. The accelerometer was placed on the V_2 position, above the xiphoid process and left to the sternum.

A MEMS accelerometer with a sensitivity level of 800 mV/g is used, where g is the acceleration due to the gravity of the Earth [semiconductor, 2011]. The sensor is mounted on a small Printed Circuit Board (PCB) which includes a circuit to amplify and filter the sensed signals from the accelerometer [semiconductor, 2011]. There can be three analog voltage outputs from its three x, y, and z-axis, as mentioned before in Section 3.2. As expected, it is found that the heart pushes felt at the chest wall, are strongest in the direction perpendicular to the chest. Due to this reason, signal only from the z-axis, perpendicular to the chest, is acquired. The z-axis signal is connected to the PC through the sound card, as shown in Figure 3.4. Power to the accelerometer is provided through USB 3.0 port of the PC. The power consumption of the accelerometer is 250 μA, which is very small as compared with the capacity of the battery (typically 5000 mAh) of the PC.

3.3.3 ECG Signal Acquisition

ECG signal is also acquired to use as a reference signal, simultaneously to the PCG and SCG signal. To acquire the ECG signal, three electrodes were attached to the left shoulder, right shoulder and left leg respectively, as shown in Figure 3.4. Such arrangement of the electrodes makes Einthoven's triangle. The electrical signal generated due to the activity of the heart is low in amplitude and gets affected due to various noises such as power line interference and baseline wandering. For the amplification and filtering of the acquired ECG signal, an application-specific integrated circuit (AD8232, Analog Devices), is used. The AD8232 consists of a signal conditioning block for ECG and other biopotential measurement applications [Analog-Devices]. It is designed to extract, amplify, and filter biopotential signals in the presence of noise, such as those created by motion.
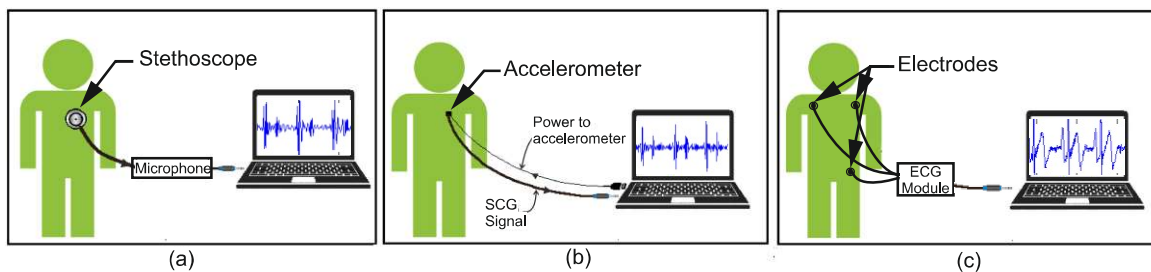

Figure 3.4 : System setup for signal acquisition using (a) PCG, (b) SCG, and (c) ECG

3.4 TIME, FREQUENCY AND TIME-FREQUENCY DOMAINS ANALYSIS OF THE PCG AND SCG SIGNALS

Both the signals are represented in the time, frequency, and time-frequency domains. Frequency domain representation is obtained by Fourier transform and time-frequency domain representation is obtained by WT. Signal analyses in each domain are described in the following subsections.

3.4.1 Time Domain Analysis

For the time domain analysis, ensemble averaging is performed on both the signals of 20 seconds duration. Ensemble averaging normalize the impact of HRV from the signal [Migeotte et al., 2014]. To perform ensemble averaging, both signals were separated in cardiac cycles (from R to R wave). Then each cycle is time aligned and time axis was normalized so that the length of the cycle set to 1000 samples. Then, normalized signals of each cycle were superimposed and averaged. The obtained curves for both the signals are shown in Figure 3.5.

Since PCG and SCG signals were acquired simultaneously, it can be observed from Figure 3.5 that the obtained location of S1 and S2 in SCG signal is the same as that of S1 and S2 in PCG signal. Cardiac events such as mitral valve closing and aortic valve closing can be extracted from both the signals. These two events correspond to first heart sound (S1) and second heart sound (S2), respectively. It demonstrates the capability of SCG to acquire the heart sound signal and its fundamental components. However, the shape of the waves related to particular cardiac events is different in both the signals.
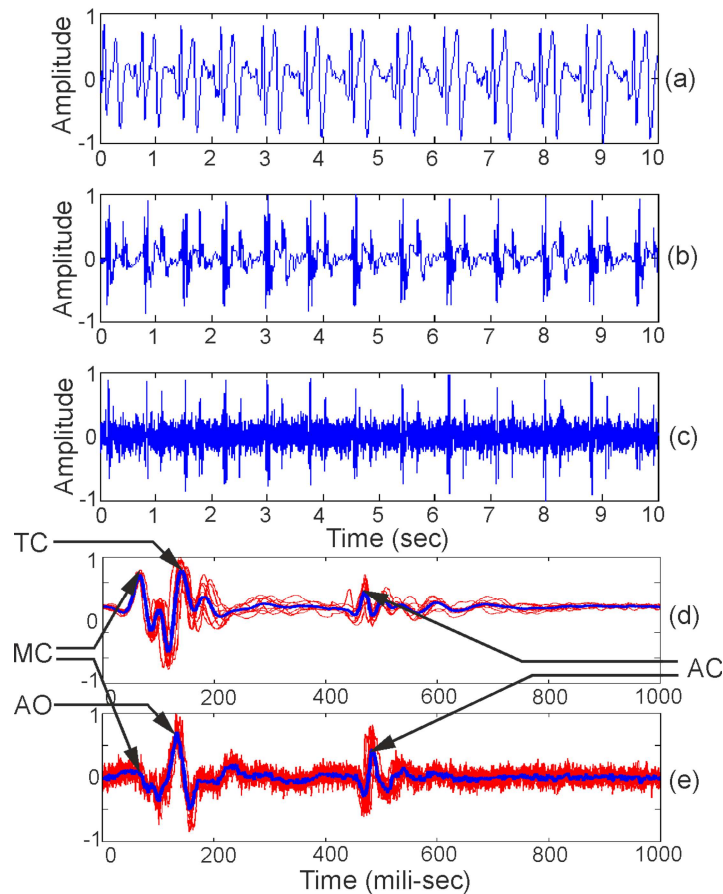

Figure 3.5 : Time domain representation of signals: (a) ECG, (b) PCG, (c) SCG, (d) Ensemble averaged PCG, and (e) Ensemble averaged SCG

3.4.2 Frequency Domain Analysis

Fourier transform is a technique to transform a time-domain signal into a frequency domain signal [Singh and Anand, 2007]. The frequency domain analysis is performed to find out dominant frequency contents in the heart sound signal. The frequency domain representation of the signal, $x(n)$, is obtained by the Fourier transform as:

$$X(R) = \sum_{n=0}^{N-1} x(n).e^{-j2\pi Rn/N}, R \in Z(integers) \tag{3.10}$$

where N is the length of the signal, $X(R)$ represents the discrete Fourier transform coefficients at frequency R for the signal $x(n)$. Frequency domain analysis of the acquired signals is performed by transforming the signal into the frequency domain using Fourier transform according to Eq.(3.10). The obtained power spectrum of the PCG signal is shown in Figure 3.6. The percentage of the power spectrum of the PCG signals of five subjects is provided in Table 3.1 in 10 Hz frequency bins. From the figure and the Table, it can be observed that more than >70% energy of the PCG signal lies in the 0-40 Hz band. This observation indicates that the observed PCG signal is a normal heart sound signal [Jain and Tiwari, 2014]. Frequency do-
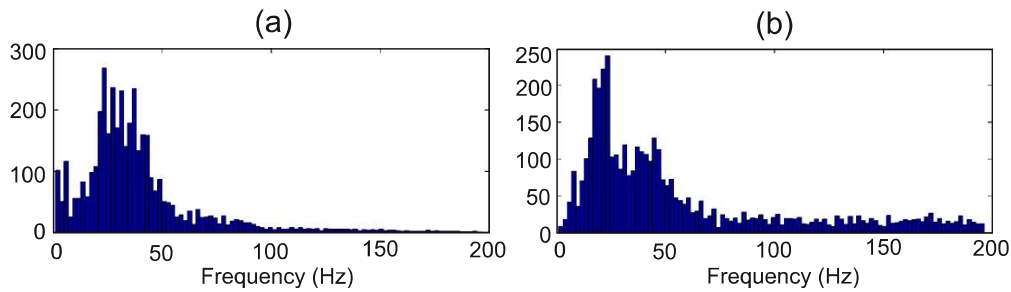

Figure 3.6 : Power spectrum of signals: (a) PCG signal and (b) SCG signal

main analysis of the acquired SCG signals of five subjects is performed. The obtained power spectrum of the SCG signal is shown in Figure 3.6 and the percentage of the power spectrum of the SCG signal of five subjects is provided in Table 3.1. From the figure and table, it can be observed that the SCG signal has more than >70% energy in the frequency band of 10-60 Hz.

Table 3.1 : Percentage power spectrum of the PCG signal in 10 Hz bins

S. No.	Frequency (Hz)					
	0-10	11-20	21-30	31-40	41-50	51-60
1	32.7	21.8	11.8	7.2	6.1	4.1
2	31.9	30.4	14.4	6.4	5.4	2.0
3	25.1	29.5	12.9	6.5	4.5	4.0
4	37.9	16.1	15.2	11.8	2.5	2.1
5	25.6	21.5	21.6	16.3	5.2	2.0

Table 3.2 : Percentage power spectrum of the SCG signal in 10 Hz bins

S. No.	Frequency (Hz)					
	0-10	11-20	21-30	31-40	41-50	51-60
1	8.4	21.4	19.4	16.9	8.5	6.1
2	7.4	11.5	16.2	12.2	11.0	6.3
3	4.4	19.9	14.0	18.5	13.3	10.8
4	5.6	17.8	16.0	18.9	8.9	7.8
5	9.5	21.4	18.4	15.9	13.1	9.4

3.4.3 Time-frequency Domain Analysis

To obtain the time location of the frequency contents, signals are analysed in the time-frequency domain. The heart sound signal has been analysed intensively using WT because it produces good time resolution at high frequencies and good frequency resolution at low frequencies [Shen et al., 2013; Reed et al., 2004; Singh and Anand, 2007]. It uses relatively smaller window size to produce good time resolution at high frequencies and larger window size for good frequency resolution at low frequencies. Continuous Wavelet Transform (CWT) can be computed by correlating the signal $x(n)$ with shifted and scaled version of the mother wavelet $\Psi_w(n)$, and it produces a set of coefficients $C(s,t)$ given by:

$$C(s,t) = \frac{1}{\sqrt{s}} \sum_{n=t-M/2}^{t+M/2} x(n)\Psi_w\left(\frac{n-t}{s}\right) \tag{3.11}$$

where M is the duration of wavelet. The factor $1/\sqrt{s}$ is introduced to guarantee energy preservation. The mother wavelet is shifted with time t and scaled by a scaling factor a, which is inversely proportional to the frequency as follows:

$$R = \frac{F_c \times F_s}{s} \tag{3.12}$$

where F_c is the centre frequency of mother wavelet $\Psi_w(n)$, and F_s is the sampling frequency of the signal $x(n)$.

In literature, it is reported that 'Coif5' wavelet gives a good analytical performance for the heart sound signal [Gradolewski and Redlarski, 2014]. It is because 'Coif5' wavelet is an orthogonal wavelet, which ensures good reconstruction of the signal, and it has compact support with highest vanishing moments which reduce computational complexity [kaur et al., 2013]. Henceforth, 'Coif5' wavelet is used to analyse both the PCG and SCG signals.

The result of time-frequency domain analysis is shown in Figure 3.7, where the time domain signal is plotted above the scalogram of wavelet coefficients. The scalogram is a visualisation method to provide a 3-D representation of the wavelet coefficients. In a scalogram, the x-axis represents time, the y-axis represents scale, which can be converted into frequency according to Eq.(3.12), and the z-axis represents the wavelet coefficient value. The coefficient value is represented by varying colours and the intensity of colours. The higher intensity means the higher value of the coefficient. The colour coding of the scalogram, used in this work, is given in Figure 3.8.

As shown in Figure 3.7, both the PCG and SCG are able to detect the FHS. In the figure, particular sections of S1 and S2 from both the signals, are magnified and plotted. From the Figure 3.7(b) it can be observed that in the PCG signal, S1 lies in the 1-27 Hz frequency band, and S2 lies in the 15-30 Hz frequency band. While, for the SCG signal (Figure 3.7(d)), S1 lies in 10-50 Hz frequency band and S2 lies in 22-62 Hz frequency band.

3.5 PERFORMANCE ANALYSIS OF PCG AND SCG SYSTEMS

To analyse the performance of both the PCG and SCG signals, the signals were recorded in 'clinical' scenario and many real-life scenarios such as when the patient was 'in meeting', 'walking', 'in motion', 'travelling', and 'in market'. As discussed previously in Section 3.3, ECG signal is also recorded simultaneously for the purpose of reference signal. The quantitative analysis of the performance of both the PCG and SCG systems is performed in two manners. First, the detection rate of the FHS components (S1 and S2) and number of false points present in the signal are obtained. Second, a quality index based on the energy of fundamental components and the rest of the cycle is proposed and obtained for both the signals
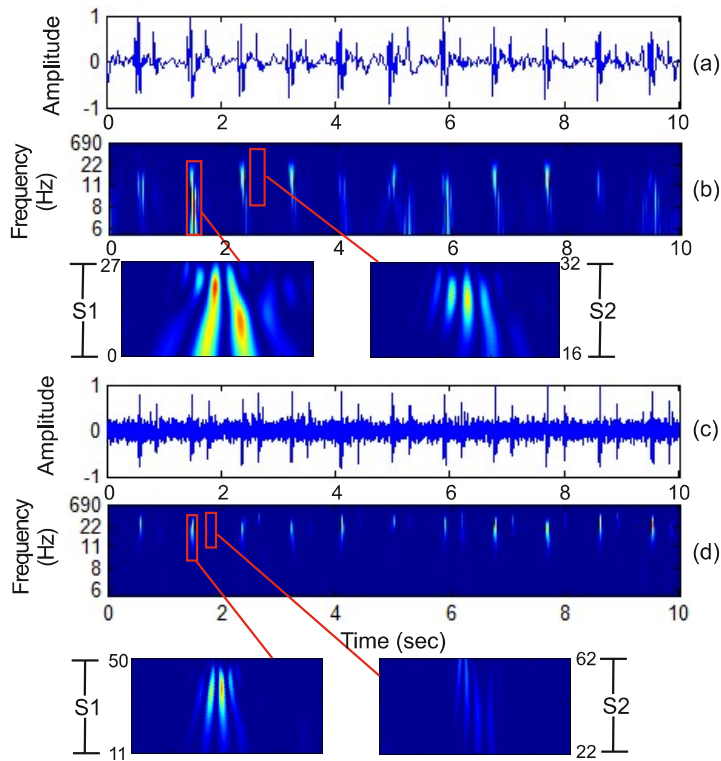
Figure 3.7 : (a) PCG signal, (b) Wavelet scalogram of PCG signal, (c) SCG signal, and (d) Wavelet scalogram of SCG signal
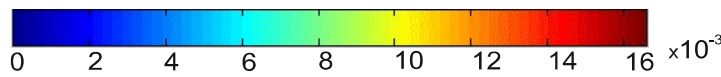

Figure 3.8 : Colour coding for the scalogram.

in all scenarios. The qualitative and quantitative analysis is provided in the following subsections.

3.5.1 Detection Rate of S1 and S2

In each scenario, ECG signal is plotted at the top and then the acquired PCG and SCG signals are plotted. Then the filtered versions of both signals are plotted. The PCG and SCG signals were filtered using a bandpass filter having frequency band 10-60 Hz. These frequency bands are set because most of the energy of the signals lies in this range, as observed in the Section 3.4. Envelopes of both the filtered signals are also obtained and plotted. The envelope is obtained using the moving average window method with window length 40 samples. Then a threshold based peak finding algorithm is applied to detect the peaks in both the signals. Separate thresholds are set manually, to detect most of the fundamental components, for both the signals in each scenario. If two peaks are detected within 150 ms, the algorithm considers larger one as a peak. This time duration is set to avoid the detection of multiple peaks for a single component. Finally, peaks are classified as S1, S2 or false point, considering ECG signal as a reference signal.

(a) Clinical Scenario

In the clinical scenario, the signals were acquired while subject sat comfortably in a peaceful environment and plotted in the Figure 3.9. From the figure, it can be observed that both the signals efficiently acquired the FHS. The same is observed for all five subjects from the Table 3.3, as the detection rate of S1 and S2 is 100 for both the signals, without any false point.
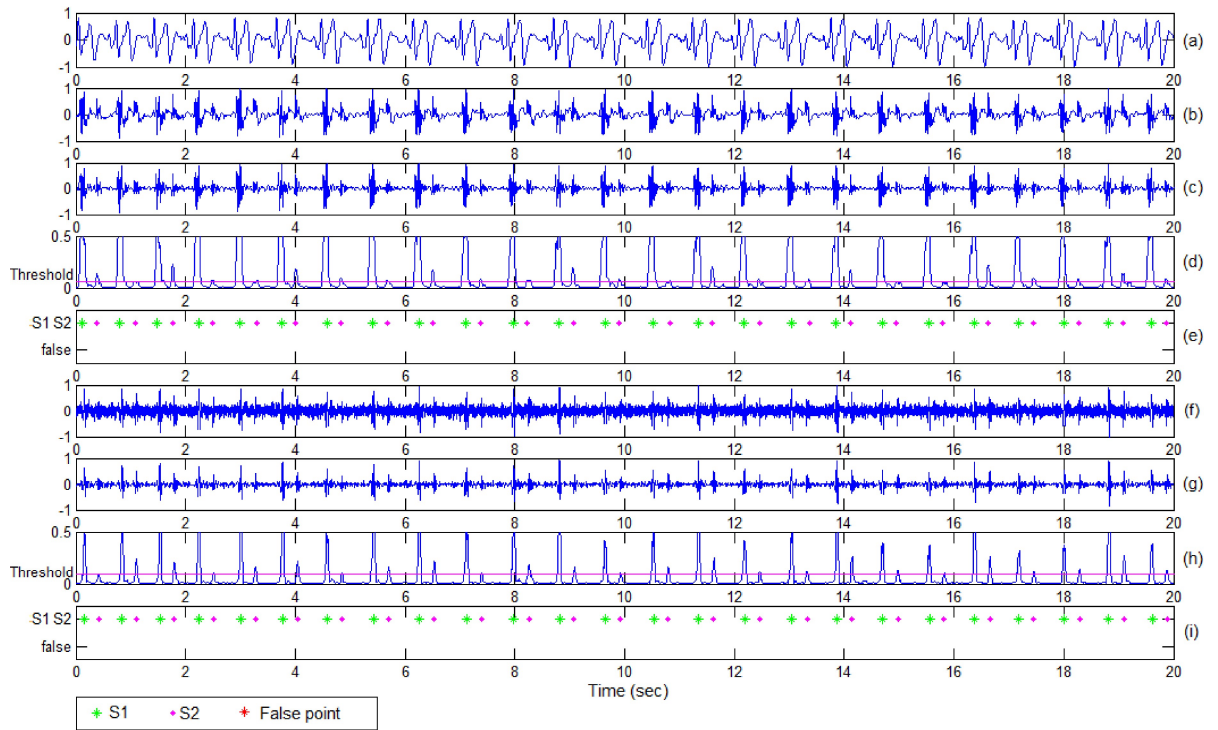

Figure 3.9 : Signals for 'Clinical' scenario: (a) ECG signal, (b) PCG signal, (c) Filtered PCG signal, (d) Averaged filtered PCG signal, (e) Detected points in PCG signal, (f) SCG signal, (g) Filtered SCG signal, (h) Averaged filtered SCG signal, and (i) Detected points in SCG signal

Table 3.3 : 'Clinical' scenario: Detection rate of S1 and S2, and number of false points detected in PCG and SCG signals

Subject	S1 (%) PCG	S1 (%) SCG	S2 (%) PCG	S2 (%) SCG	False PCG	False SCG
1	100	100	100	100	0	0
2	100	100	100	100	0	0
3	100	100	100	100	0	0
4	100	100	100	100	0	0
5	100	100	100	100	0	0

(b) In Meeting

In a daily-life scenario, a person participates in a number of meetings at home or at work place. In a meeting scenario, prominent sources of noise are 1) speech of the subject him/her self and 2) speech of other persons in the meeting. To analyse the impact of these noises, heart sound signals from both the techniques were acquired when the subject was in a meeting with three persons and they were interacting.

The ECG, PCG, and SCG signals of 'in meeting' scenario are shown in Figure 3.10. Time durations (in seconds) from 5 to 6, 11 to 12.4, 13 to 14, and 15.2 to 17.6, are the periods,

where the subject was speaking. From the figure, it can be observed that both the signals get contaminated by noise generated due to speech of the subject. However, most of the contamination is out of the frequency band of the heart sound signal components. These components can be attenuated efficiently, with the help of an appropriate band-pass filter.

From the Table 3.4, it can be observed that both PCG and SCG are able to acquire heart sound signals in the presence of speech noise. However, the number of false points detected in PCG signal is larger when compared to the false points detected in SCG signal. Furthermore, the detection rate of S1 and S2 is lower in PCG signal compared to the detection rate of S1 and S2 in SCG signal. This is due to the microphone, used to convert sound signal obtained from the stethoscope into an electrical signal. While in case of SCG, it does not require the microphone and hence it is not affected. This makes SCG a robust technique to acquire heart sound signal in the presence of noise caused by the speech of patients or other persons.
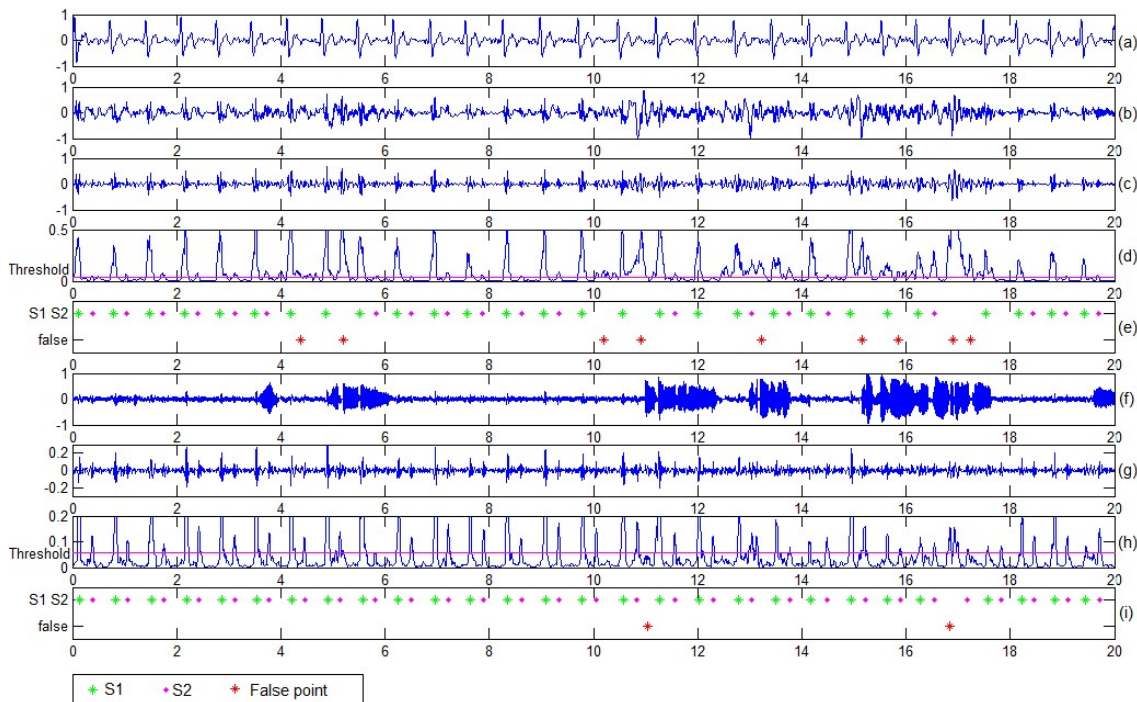

Figure 3.10 : Signals for 'in meeting' scenario: (a) ECG signal, (b) PCG signal, (c) Filtered PCG signal, (d) Averaged filtered PCG signal, (e) Detected points in PCG signal, (f) SCG signal, (g) Filtered SCG signal, (h) Averaged filtered SCG signal, and (i) Detected points in SCG signal

Table 3.4 : 'In meeting' scenario: Detection rate of S1 and S2, and number of false points detected in PCG and SCG signals

Subject	S1 (%)		S2 (%)		False	
	PCG	SCG	PCG	SCG	PCG	SCG
1	96	96	69	100	9	2
2	94	100	62	94	7	2
3	96	100	74	96	6	2
4	100	100	70	100	6	1
5	96	96	62	96	10	4

(c) Walking

When the heart is being monitored for the long-term at home or at the workplace, the patient often walks here and there. The analysis of heart sound signal during the walking is generally used to measure the ability of the heart to respond to external stress in a controlled clinical environment. This process is referred as treadmill test. Moreover, medical fraternities always advise to have a 30-minute walk on each day, to the patients with CVDs or who are prone to CVDs. The acquired signals while the subject was walking are shown in Figure 4.18. The PCG signal is contaminated due to the noise caused by footsteps as well as due to the motion of the subject. While, in the case of the SCG signal, the small size and light weight accelerometer is better attached to the body, as compared to the stethoscope. Better attachment of the sensor assures lower impact of motion and thus the lower impact of noise. However, at time instances (in second) 3.2, 4.4, 5.4, 6.3, 7.1, 8.2, 9.3, 10.2, 11.6, 12.5, 16.5, 17.7, 18.6, and 19.7, due to a footstep, there is an extra component (noise) present in the SCG signal. The footsteps cause vibration on the body and chest wall, and these vibrations contaminate the heart sound components.

From the Table 3.5, for 'walking' scenario, it can be observed that the detection rate of S1 is lower of the PCG signal when compared to the detection rate of S1 of the SCG signal. The rate further decreases for the detection of S2 in PCG signal. The number of false points detected in PCG signal is also larger than the number of false points detected in the SCG signal for all subjects.
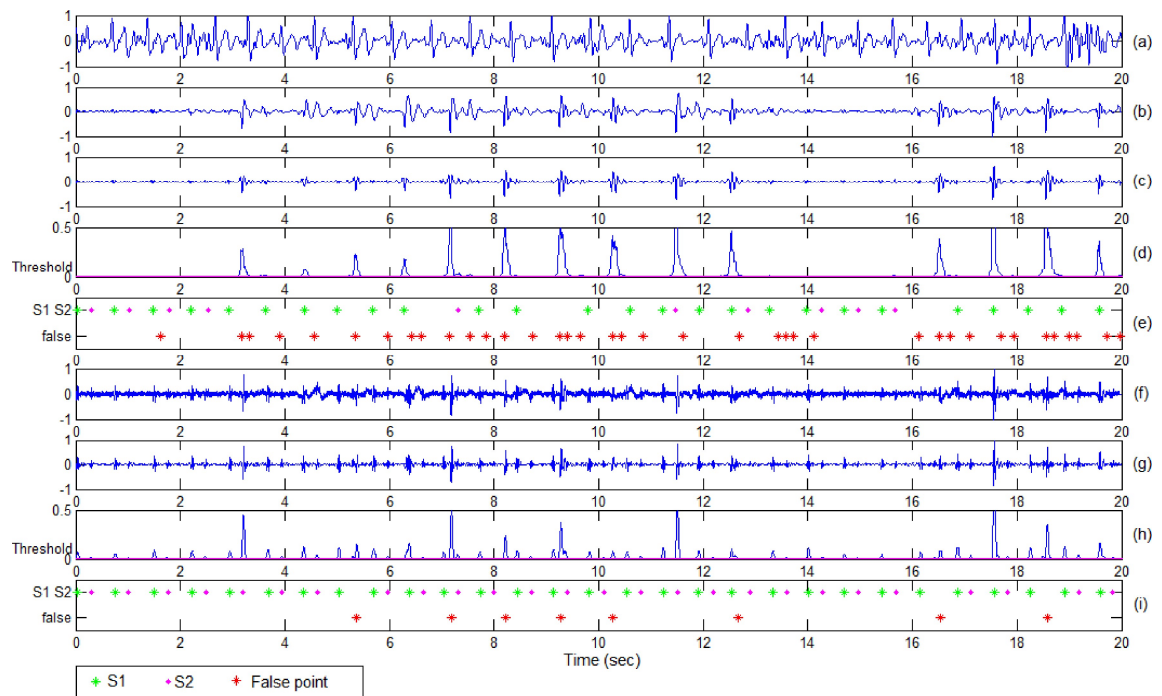

Figure 3.11 : Signals for 'walking' scenario: (a) ECG signal, (b) PCG signal, (c) Filtered PCG signal, (d) Averaged filtered PCG signal, (e) Detected points in PCG signal, (f) SCG signal, (g) Filtered SCG signal, (h) Averaged filtered SCG signal, and (i) Detected points in SCG signal

(d) Motion of Patient

While monitoring the heart for a long-time at home, it is difficult to avoid motion of the patient. Thus, it is important to analyse the performance of both the systems in the case

Table 3.5 : 'Walking' scenario: Detection rate of S1 and S2, and number of false points detected in PCG and SCG signals

Subject	S1 (%) PCG	S1 (%) SCG	S2 (%) PCG	S2 (%) SCG	False PCG	False SCG
1	76	96	27	88	44	8
2	72	92	32	82	38	9
3	67	88	27	86	32	6
4	65	92	25	78	39	8
5	54	90	22	66	52	10

of motion of the patient. Figure 3.12 shows that SCG signal is more robust to motion noise, as compared to the PCG signal. PCG signal gets affected significantly due to the motion of the subject. The robustness of the SCG is due to the good attachment of its sensor to the body, same as in 'walking' scenario. From Table 3.6, it can be observed that the detection rate of S1 and S2 of the SCG signal is large as compared with the detection rate of S1 and S2 in the PCG signal. Further, the number of false points detected in SCG signal is low as compared with the false points detected in PCG signal.
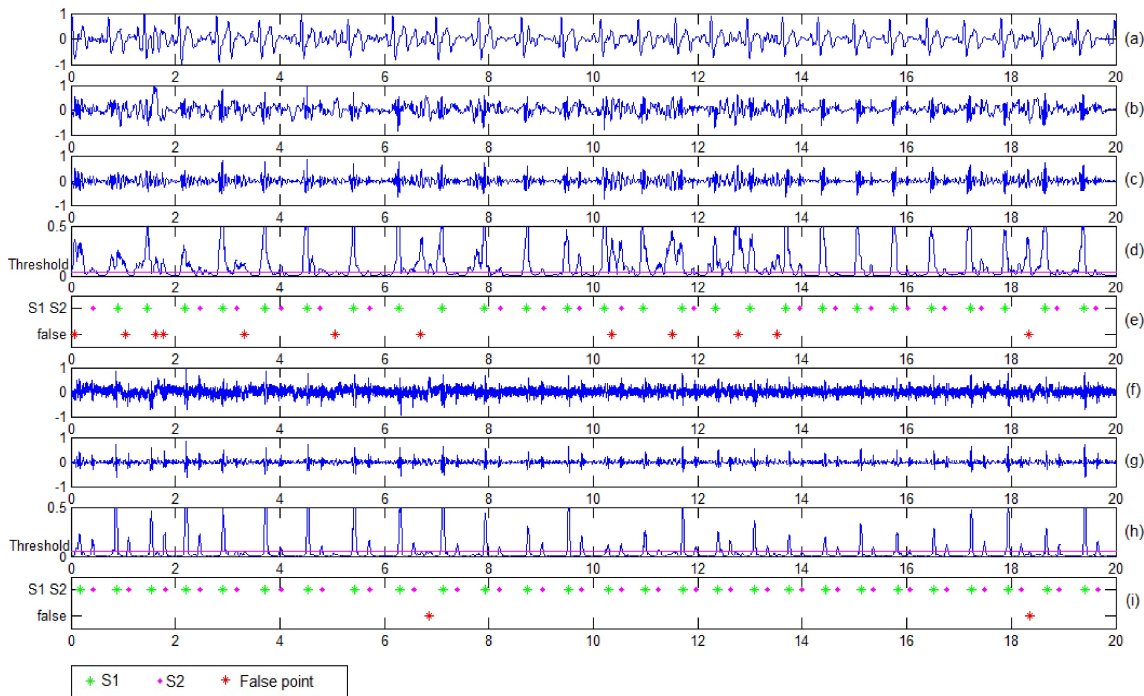

Figure 3.12 : Signals for 'motion of patient' scenario: (a) ECG signal, (b) PCG signal, (c) Filtered PCG signal, (d) Averaged filtered PCG signal, (e) Detected points in PCG signal, (f) SCG signal, (g) Filtered SCG signal, (h) Averaged filtered SCG signal, and (i) Detected points in SCG signal

(e) Travelling

According to the survey report [for transport U.K., 2012], people spent an average of 361 hours per year travelling. Thus, it would be beneficial, if heart can be monitored while the subject is travelling. Therefore, in this case also, the heart sound signals were acquired using both the techniques while the subject was in a moving car on a plane road. The acquired signals are shown in Figure 3.13. From the figure, it can be observed that signals of both

	S1 (%)		S2 (%)		False	
	PCG	SCG	PCG	SCG	PCG	SCG
Sub 1	93	100	70	100	13	2
Sub 2	91	100	68	100	17	8
Sub 3	88	100	71	100	16	5
Sub 4	90	96	65	94	21	8
Sub 5	93	100	68	100	16	6

the techniques get contaminated due to the noise caused by vibration of the car. Although, from the filtered versions (Figure 3.13(b) and Figure 3.13(g)), it can be observed that SCG signal is less affected when compared to the PCG signal. As discussed in introduction Section, frequency response of stethoscope is not flat and hence get affected significantly due to noise. While, due to flat frequency response of the accelerometer, SCG signal was able to acquire heart sound signal while the subject was travelling. However, at time instances 4 second and 11 second, there were bumps on the road and due to them, SCG signal also gets affected significantly.

It can be observed from the Table 3.7, that SCG signal is more robust than the PCG signal. The detection rate of S1 and S2 in SCG signal is higher than the detection rate in PCG signal. Furthermore, the number of false detected points in PCG signal is larger than the number of false detected points in SCG signal.
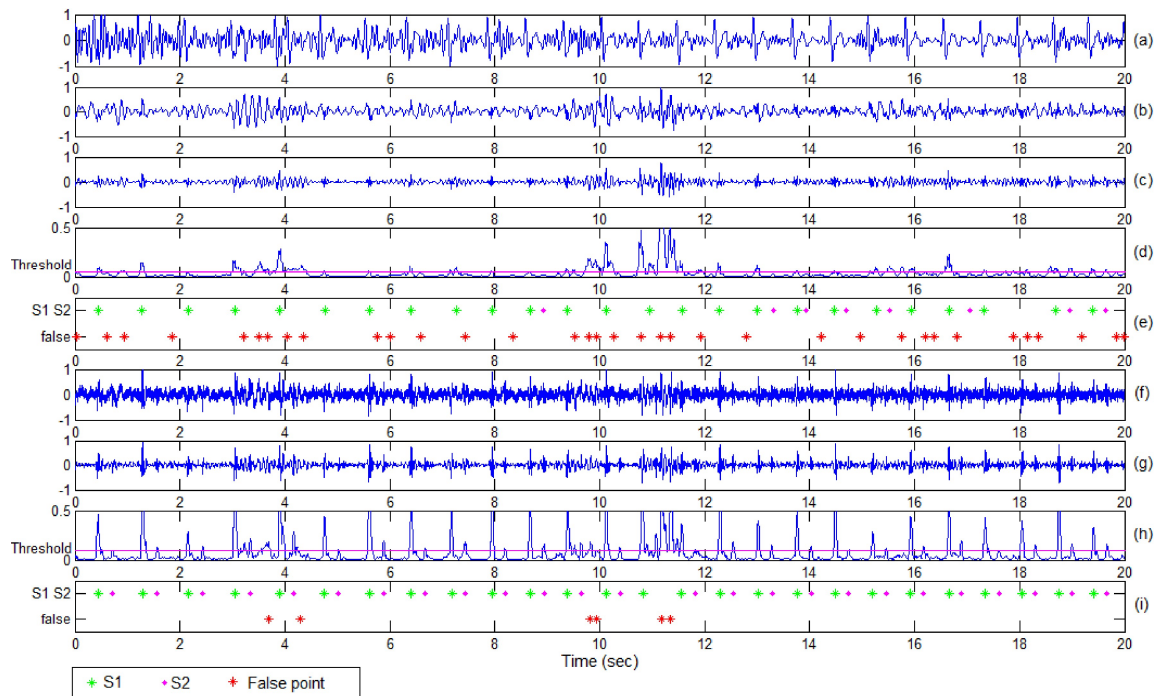

Figure 3.13 : Signals for 'travelling' scenario: (a) ECG signal, (b) PCG signal, (c) Filtered PCG signal, (d) Averaged filtered PCG signal, (e) Detected points in PCG signal, (f) SCG signal, (g) Filtered SCG signal, (h) Averaged filtered SCG signal, and (i) Detected points in SCG signal

Table 3.7 : 'Travelling' scenario: Detection rate of S1 and S2, and number of false points detected in PCG and SCG signals

Subject	S1 (%)		S2 (%)		False	
	PCG	SCG	PCG	SCG	PCG	SCG
1	88	100	19	96	40	6
2	84	96	46	88	31	4
3	81	100	61	96	28	3
4	65	92	23	69	43	9
5	73	92	31	81	36	7

(f) In Market

Market is a scenario where a number of external sound noise sources are present such as vehicle noise, loud-speaker noise, and people's screaming. This scenario represents many scenes, including typical vegetable markets, railway-stations, and bus-stations. As before, we recorded both the PCG and SCG signals at a railway-station and analysed them.

The ECG, PCG and SCG signals acquired at railway-station are shown in Figure 3.14. Both the PCG and the SCG systems are able to acquire heart sound signal. From the Table 3.8, it can be observed that S1 is detected in both the signals with 100 % accuracy. However, the detection rate of S2 is low in the PCG signal as compared with the detection rate of S2 in SCG signal. Further, the number of false detected points is larger in PCG signal than the SCG signal.
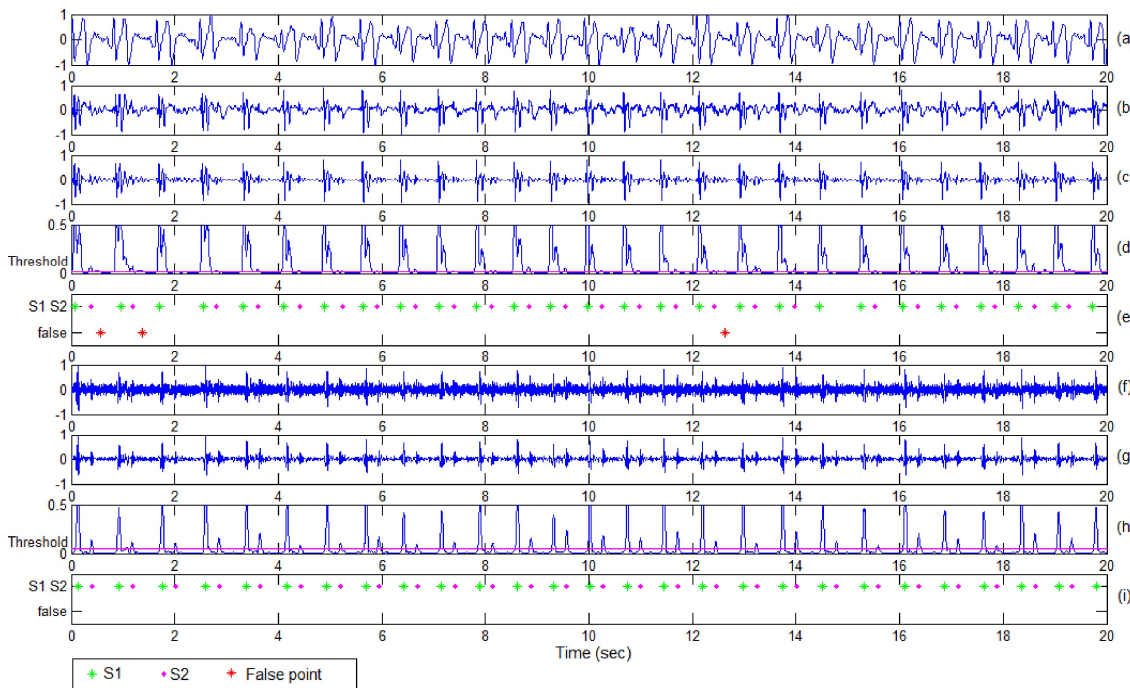

Figure 3.14 : Signals for 'in market' scenario: (a) ECG signal, (b) PCG signal, (c) Filtered PCG signal, (d) Averaged filtered PCG signal, (e) Detected points in PCG signal, (f) SCG signal, (g) Filtered SCG signal, (h) Averaged filtered SCG signal, and (i) Detected points in SCG signal

Table 3.8 : 'Market' scenario: Detection rate of S1 and S2, and number of false points detected in PCG and SCG signals

| Subject | S1 (%) | | S2 (%) | | False | |
	PCG	SCG	PCG	SCG	PCG	SCG
1	100	100	92	100	3	0
2	100	100	96	100	5	0
3	100	100	88	96	7	1
4	100	100	92	100	5	0
5	100	100	92	100	4	0

3.5.2 Quality Index Based Performance Analysis

A quality index for heart sound signal is proposed based on the energy of FHS and the rest of the cardiac cycle (silence period). To obtain the quality index, first, both signals were filtered using a bandpass filter having frequency band 10-60 Hz. Then, S1 and S2 are detected with the help of ECG signal and separated as shown in Figure 3.15(c) and Figure 3.15(f) for PCG and SCG signal respectively, in 'clinical' scenario. Rest part of the signal (excluding S1 and S2) is shown in Figure 3.15(d) and Figure 3.15(g) for the PCG and the SCG respectively. Finally, the quality index is obtained as follows:

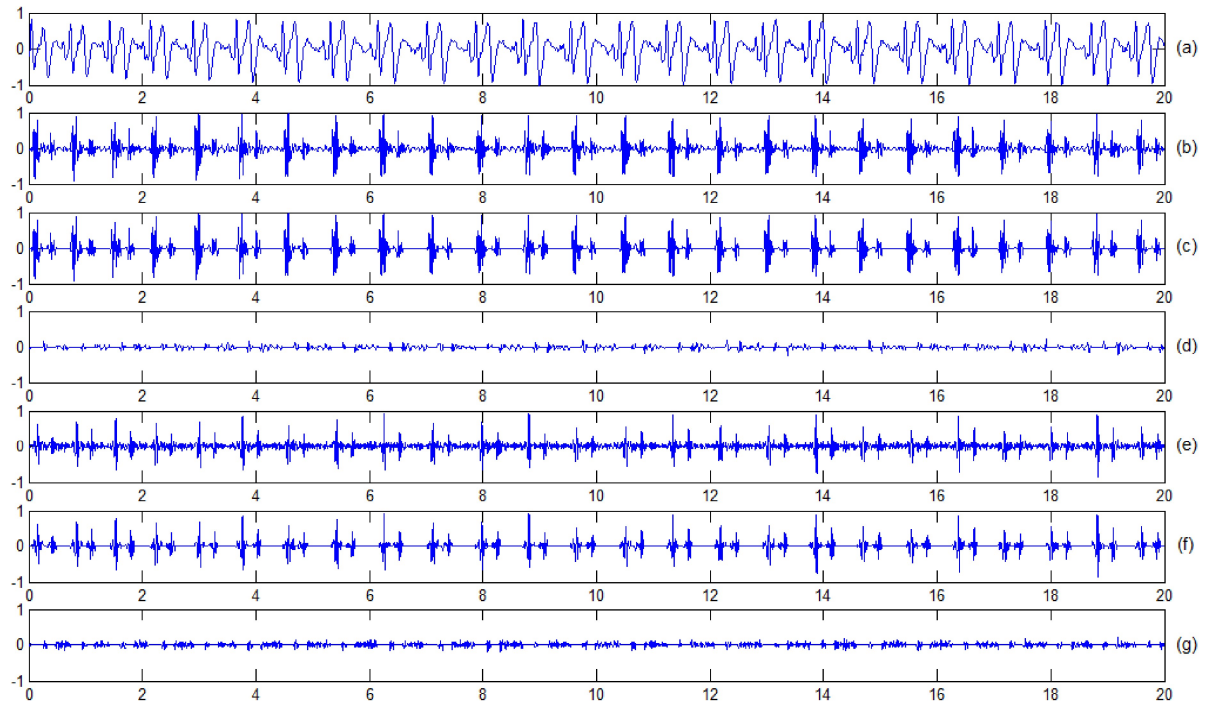$$Q_i = \frac{\text{energy of S1 and S2}}{\text{energy of rest of cycle}} \qquad (3.13)$$

Figure 3.15 : 'Clinical scenario' signals: (a) ECG signal, (b) Filtered PCG signal, (c) S1 and S2 in PCG signal, (d) Rest of the cycle in PCG signal, (e) Filtered SCG signal, (f) S1 and S2 in SCG signal, and (g) Rest of the cycle in SCG signal

The obtained quality indices for both the PCG and SCG signals in different scenarios are provided in Table 3.9. In 'clinical' and 'market' scenarios, the quality index of the SCG

signal is lower when compared to the quality index of the PCG signal. These two scenarios are where both signals do not get affected due to noise, as analysed previously. The quality index of SCG signal in these scenarios is low because the energy of silent period (rest of the cycle) in SCG signal is higher than the energy of the silent period in PCG signal. It demonstrates that PCG is a more suitable device than SCG to record heart sound signal in the clinical environment.

Scenarios where the noise was present, the quality index for the SCG signal is larger than the quality index for the PCG signal. The quality index of SCG signal does not degrade significantly in noisy scenarios compared to the quality index of SCG signal in 'clinical' scenario. On the other hand, scenarios such as 'walking' and 'travelling', where the signals get affected significantly, the quality index of PCG signal is degraded more than 200% compared with the quality index of PCG signal in 'clinical' scenario. It indicates that the PCG signal gets affected significantly in the presence of noise, while SCG signal is less impacted by the presence of noise.

Table 3.9 : Quality index for PCG and SCG signal in different scenarios

Subject	Clinical		Walking		Meeting		Travelling		Market	
	PCG	SCG	PCG	SCG	PCG	SCG	PCG	SCG	PCG	SCG
1	3.6113	2.4634	1.1567	2.0860	2.4569	2.3695	1.0339	1.6516	3.3880	2.8270
2	3.4129	2.8251	1.0253	2.1025	2.6874	2.6521	0.9562	1.7452	3.1822	2.9126
3	3.7011	2.8821	1.2031	2.2090	2.5263	2.4568	1.1245	1.6852	3.1569	2.8549
4	3.3256	2.7846	1.3540	2.2560	2.8632	2.7489	1.0256	1.4585	3.0130	2.7251
5	3.4563	2.8546	0.9865	1.9374	2.3547	2.1459	0.9214	1.5317	3.1593	2.6138

3.6 CONCLUSIONS

In this chapter, the performance of both the PCG and SCG systems are analysed in clinical and various real-life scenarios. The recorded signals using both the systems are analysed in time, frequency, and time-frequency domain. Time and time-frequency domain analysis demonstrate the correlation between the heart sound components in the PCG signal and in the SCG signal. This analysis shows the ability of SCG to acquire diagnostically important heart sound signal components. Furthermore, we compared the performance of both the systems qualitatively and quantitatively, in the presence of noise.

Observations of the qualitative and quantitative performance analysis show that the SCG signal is more robust to noise as compared to the PCG signal. There are three shortcomings of the PCG systems. First, it uses a microphone to convert the acoustic sound signal, acquired using a stethoscope, into an electrical signal. Use of microphone makes it susceptible to environmental noise. Second, the large size and heavy weight of its sensor cause a disturbance in the signal during its acquisition by the sensor attached to the body of the subject in motion. Third, the frequency response of the stethoscope is not flat in the frequency range of interest. On the other hand, SCG does not require a microphone, and small size and light weight of its sensor are in favour of good attachment to the chest wall. Further, the accelerometer has a relatively flat frequency response. These merits make the SCG signal robust to various noises, although there is a scope of suppression of in-band noise from the SCG signal. Moreover, in 'walking' scenario, the presence of extra components (noise) is observed in the SCG signal due to footsteps. The analysis of the signal in 'walking' scenario is more important as it is used to measure the heart's ability to respond to external stress.

The findings of this chapter conclude that PCG can be replaced by SCG to acquire the heart sound signal for long-term monitoring in real-life scenarios. The requirement of an efficient denoising algorithm is also observed to remove in-band noise from the heart sound

signal components. Therefore, in the next chapter, a DWT based denoising algorithm is presented to remove the in-band noise from the heart sound signal. Moreover, in view of the importance of analysis of the signal in the walking scenario, a noise removal algorithm using multiple axes of an accelerometer is also presented in the next chapter.

…